Cureus Journal of Engineering

Open Access Original Article

Fabrication and Microstructural Analysis of SUS316-Al2O3 Functionally Graded Beams Manufactured using Plasma Thermal Spray Technique

Pravin Malik [1] , Ravikiran Kadoli [1]

1. Department of Mechanical Engineering, National Institute of Technology Karnataka Surathkal, Mangalore, IND

Corresponding author: Pravin Malik, pravin_malik@yahoo.com

Received 05/17/2025
Review began 06/02/2025
Review ended 06/18/2025
Published 07/14/2025

DOI: https://doi.org/10.7759/s44388-025-03743-5

Abstract

This study investigates the development of functionally graded materials (FGMs) designed to possess a combination of high temperature resistance and high strength, with potential applications in defense, aerospace, energy, and medical sectors. Specifically, the research focuses on fabricating functionally graded beams composed of SUS316 and Al_2O_3 using the plasma spraying technique with ceramic content varying from 0 to 40% at the outermost surface. The research involves parametric optimization to determine the ideal process parameters for FGM beam fabrication. Potential defects such as porosity and voids identified during sample preparation were addressed through targeted corrective measures, including controlling the relative speed of the spray gun and adjusting the coating thickness with each pass. A detailed microstructural analysis, conducted using scanning electron microscopy, reveals a layered gradation of materials within the plasma-sprayed beams, with distinct distribution patterns of the constituent elements.

Categories: Advanced Manufacturing Technologies, Advanced Materials, Materials Engineering
Keywords: functional material, ceramic composites, microstructure, plasma spraying, alumina, sus316

Introduction

The evaluation of thermal strain and stress is a crucial aspect of the design process for systems such as gas turbine, nuclear reactor assembly, aerospace components, chemical reactors, and electronic circuit boards. When structural elements such as frames, outer coverings, or enclosures are exposed to surface heating, temperature gradients develop in different directions within the material. These thermal gradients can lead to thermal distortion, thermal sag, and mechanical interference, which may result in malfunction or operational failure. During last two decades, researchers have started focusing on functionally graded materials (FGMs) characterized by gradual spatial variation in their composition, leading to corresponding changes in their properties [1,2]. FGMs composed of ceramic on the outer surface and metal on the inner surface, and a gradual transition between ceramic and metal in the intermediate layers, are highly effective at reducing mechanical and thermal stress concentration. For example, during re-entry into Earth's atmosphere, the space shuttle uses ceramic tiles for thermal protection to withstand intense heat generated [3]. The silica tiles are bonded on to the aluminum stiffened super structure of the shuttle. The silica tile expands at a different rate than the underlying aluminum structure it is protecting. This difference in thermal expansion between silica and aluminum creates stress concentrations at the interface between the tile and substructure, potentially leading to cracking or delamination of the tile. The ceramic tiles can be replaced by FGM tiles with inner material similar to superstructure and outer material as ceramic.

Lambros et al. [4] introduced an innovative method for fabricating and conducting fracture tests on large-scale polymer-based FGMs. Similarly, Mahamood et al. [5] provided a comprehensive review of fabrication techniques, application areas, and recent research developments related to FGMs. They classified FGMs into two main categories: thin and bulk FGMs. Thin-section or surface coating FGMs are created through methods such as chemical vapor deposition, physical vapor deposition, and plasma spraying, while bulk FGMs are produced using techniques like solid freeform fabrication, centrifugal casting, and powder metallurgy. Sobczak and Drenchev [6] carried out an extensive review of the core manufacturing methods for metal-based FGMs, presenting several previously unpublished findings. They showed that it is possible to create FGMs with customized gradient variations to suit the specific needs of various engineering applications. Mondal et al. [7] offered a brief review on the current status of thermal barrier coatings, highlighting recent advancements in their fabrication and performance, addressing their limitations, and providing recommendations for their future use in extreme high-temperature environments. Ju et al. [8] analyzed recent developments in research on steel-based FGMs, categorizing them by material and gradient types, and discussed the challenges and issues related to these materials. Saleh et al. [9] provided an overview of design and manufacturing techniques for smooth graded FGMs, outlining the key challenges and advantages of these methods based on over 30 years of available literature.

Among the various processes used to fabricate graded materials, thermal spray stands out as one of the most suitable techniques for producing gradient materials due to its versatility and excellent microstructural control. Numerous studies have explored the fabrication of metal-ceramic gradient materials, specifically using alumina as the ceramic component, through different plasma spraying methods. Ctibor et al. [10] employed the water-stabilized plasma (WSP) spray and gas-stabilized plasma (GSP) spray processes to create composite coatings from a blend of stainless-steel powders and alumina-based ceramic. Gu et al. [11] utilized the plasma spray technique to fabricate functionally graded ZrO_2-NiCrAlY coatings, using pre-mixed spheroidized powders as feedstock. The chemical homogeneity and consistent density across the layers is achieved by use of pre-mixed powders. Amsellem et al. [12] studied the microstructure of a range of composites fabricated using air plasma spraying (APS) alumina. Zhang and Kobayashi [13] investigated the corrosion resistance of Al_2O_3 + ZrO_2 composite coatings applied to stainless steel substrates using a gas tunnel-type plasma spraying process. Li and Sun [14] examined the properties and microstructure of Al_2O_3 coatings deposited with a novel hollow cathode microplasma torch. Using the combustion powder thermal spray process, Kapuria et al. [15] fabricated the five-layered Ni-Al_2O_3 FGM beam samples. The static bending and free vibration behavior studies using experimental and theoretical investigations of SUS316/Al_2O_3 FGM beams, fabricated using plasma spraying techniques, have been performed by Malik et al. [16]. Bhattacharyya et al. [17] fabricated multilayered FGM Ni/Al_2O_3 and Al/SiC beams using the thermal spraying technique and powder metallurgy process, respectively. Wattanasakulpong et al. [18] developed a theoretical model based on third-order shear deformation theory to analyze the free vibrations of Al_2O_3/epoxy FGM beams, which were produced using a multi-step sequential infiltration technique. Discrepancies between the theoretical and experimental results were observed, primarily due to porosities introduced by imperfect infiltration and the approximations made in the material model. Parihar and Maitra [19] conducted studies on the design optimization of a rotating truncated conical shell made from FGM, subjected to both variable and constant internal pressures, using the Finite Element Method. Williams et al. [20] reviewed several recent patents on the spark plasma sintering process, particularly those related to electromagnetic functional materials, nanomaterials/composites for mechanical applications, thermoelectric materials, and fuel cell components.

Grammes et al. [21] presented a combined analysis of hardness profiles through indentation and microstructure of functionally graded tungsten/steel coatings, which were plasma sprayed onto steel substrates. Experimental studies conducted by Ortega-Bautista et al. [22] investigated the effect of powder characteristics, such as chemical composition, on the deposition of ceramic coatings on PEEK substrates. Their findings demonstrated that the surface of PEEK can be successfully functionalized, transforming it from an inert material to one displaying bioactivity through the application of a HA-based bilayer or multilayered coating. Audouard et al. [23] investigated the Spark Plasma Sintering (SPS) of fully stabilized hafnia with yttrium oxide (yttria) to understand the impact of manufacturing parameters on the crystallography, chemistry, and microstructure of the material. Kim et al. [24] additively manufactured a FGM composed of a Ni-based Inconel superalloy (Inconel 718) and Fe-based stainless steel (SS 316L) via directed energy deposition (DED). They evaluated the microstructural transformation, defect behavior, and Vickers hardness of the material, observing these properties as a function of the discrete chemical composition, which varied in steps of 10 wt% of the two materials along its length. Guo et al. [25] fabricated tungsten-armored first wall composite coatings of W-316 L steel (WSS) on 316 L steel substrates using detonation spraying (DS) to investigate their main characteristics and performance under transient heat shocks. Goudarzi et al. [26] designed and optimized the structure of a thick thermal barrier coating by incorporating graded layers to achieve a balance between high thermal insulation capacity and durability, which was fabricated using APS. Singh et al. [27] formulated a functionally graded coating (FGC) in three successive layers over Ti_6Al_4V alloy using an APS process. Muniraj and Sreehari [28] investigated the structural response, energy absorption, and damage mechanisms of Al/SiC functionally graded plasma-sprayed face plates and aluminium honeycomb cores subjected to single and repeated impacts. Matějíček et al. [29] fabricated tungsten-steel composites and FGMs using a high-power hybrid water-argon plasma spraying system.

In recent years, researchers have focused on the understanding and developing the manufacturing processes and deposition materials necessary to produce FGMs with a smooth gradation of properties. This study investigates in detail the use of plasma spraying technique for fabrication of functionally graded SUS316-Al_2O_3 beams. To study the material gradation, the microstructure studies are performed on FGM powders and FGM beam samples using scanning electron microscopy (SEM). These samples are further used for characterization of thermal and structural properties of FGM beam samples.

Materials And Methods

Material gradation across the thickness of the FGM beam

The FGM structure is regarded as a laminate composed of multiple layers of isotropic materials perfectly bonded, where each layer has a distinct composition of metal and ceramic, different compared to adjacent layers. As shown in Figure 1, consider a beam of length L having rectangular cross section. The mid-plane of the beam defines x-coordinate, the y-coordinate is along the width of the beam, b, while the z-coordinate is across the thickness (or height, h) of the beam. The metal and ceramic volume fraction follows a power law distribution, combined with the simple rule of mixtures. The material properties are considered to vary along the thickness direction of beam, with the top surface being pure ceramic and the bottom surface of pure metal.

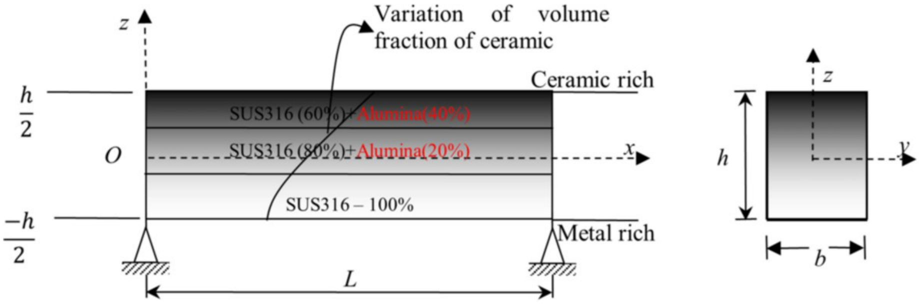

FIGURE 1: Geometry of a typical three-layer FGM fabricated of SUS316 and Al2O3

FGM, functionally graded material

The power law index, n, is always greater than or equal to zero. For different values of n, varying volume fractions of metal can be obtained. The variation of ceramic volume fraction, V_c, with power law index, n, and thickness coordinate, z/h, is shown in Figure 2. From Figure 2, it is worth noting that n = 1 follows the linear curve. Effective material properties are calculated based on the volume fraction of ceramic or metal in a particular layer. The effective material property variation across thickness is given by the relation:

$$P_{eff}(z) = (P_c - P_m)\left(\frac{z}{h} + \frac{1}{2}\right)^n + P_m \qquad (1)$$

where subscript c and m in Equation (1) denote the material property of pure ceramic and metal. The material properties for each layer vary as per the rule of mixture along the z direction.

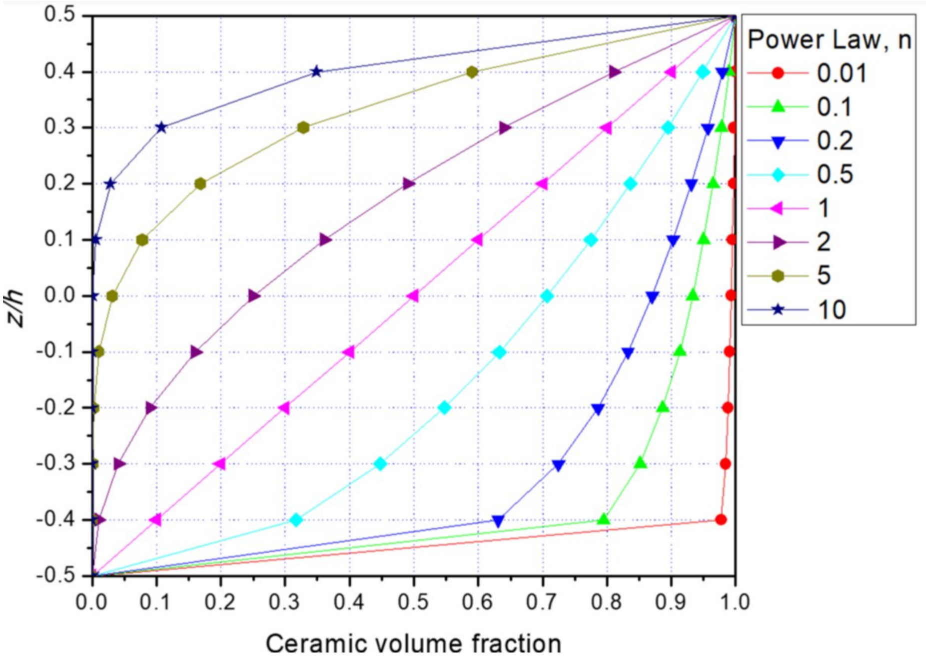

FIGURE 2: Variation of ceramic volume fraction with power law index and thickness coordinate

For each layer having a mixture of metal and ceramic with volume fractions V_m and V_c, the simple rule of mixture (ROM) is given by

$$V_c + V_m = 1 \qquad (2)$$

The power law equation is the most popular model used to describe the volume fraction variation of either metal or ceramic in designing of FGMs. In the present study, the power law equation is modified so that the volume fraction of outermost layer of ceramic will be based on the actual percentage of volume fraction of ceramic (i.e. 40%) in FGM powder rather than considering 100% ceramic. The effective material property, P_{eff} for each layer of the stepwise graded FG beam is given as

$$P_{eff}(z) = P_m V_m(z) + P_c V_c(z) \qquad (3)$$

The volume fraction of ceramic or metal is governed by power law index according to Equation (1) wherein the volume fraction is defined by

$$V_c = \left(\frac{z}{h} + \frac{1}{2}\right)^n \qquad (4)$$

Equation (1) works well when an extreme surface of the beam has the 100% volume fraction of ceramic. When the ceramic rich surface is less than 100%, the appropriate volume fraction distribution based on power law distribution is modified as

$$V_{cF} = \left(\frac{z}{h} + \frac{1}{2}\right)^n V_{cMax} \qquad (5)$$

where V_{cMax} is the maximum volume fraction of ceramic present in the material.

Fabrication of functionally graded material beams

Thermal spray and powder metallurgy have been the most widely used processes for fabricating FGMs. These processes are recognized for their versatility and excellent microstructure control. Thermal spray coatings are very reliable and can produce material coatings having minimum porosity less than 1% and coating thickness can be tailored to as thin as 0.075 mm when compared with the conventional technologies such as powder metallurgy. FGM beam samples of SUS316-Al_2O_3, consisting of multiple layers with varying volume fractions of metal-ceramic combinations, were fabricated for experimental investigation using the thermal spray process. The raw materials included 100% pure SUS316 powder with a 63-μm particle size and 99.9% pure Al_2O_3 powder with 15/45-μm size. A 0.6-mm thick SUS316 plate was used as the substrate onto which SUS316-Al_2O_3 mixture in powder form was sprayed. During the preparation of sample by thermal spray system, the thickness of individual layer was approximately maintained as 0.1 to 0.2 mm. The material properties variation is considered along the thickness direction. The ceramic content in each layer of the FGM beam samples was varied linearly from 0% to 40%, based on a power law index of n = 1 with the pure SUS316 metal base, middle layer with 20% ceramic content and the top layer having 40% ceramic content. The material was meticulously sprayed across the substrate surface to achieve uniform thickness. The details of the samples prepared using thermal spray process used in the present study are given in Table 1. The sample used in present study was 150 mm long, 30 mm wide and had an average thickness of 0.925 mm.

Sample no.	No. of layers	Volume fraction of metal and ceramic (%)			Length "L", mm	Thickness "h", mm	Width "b", mm
		1	2	3			
1	3	100:0	80:20	60:40	150	0.925	30
2	3	100:0	80:20	60:40	180	0.75	17.5
3	3	100:0	80:20	60:40	180	0.78	30
4	2	100:0	0:100	-	150	0.72	30

TABLE 1: Details of the fabricated SUS316-Al2O3 FGM beam samples

FGM, functionally graded material

Powder mixing

Two SUS316/Al_2O_3 stock mixtures, with 20% and 40% ceramic volume fractions, were prepared, and mechanical alloying was performed in a high-energy planetary ball mill (RETSCH PM-100, Figure 3). Stainless steel milling container and tungsten carbide balls were used for mixing. The number of tungsten carbide balls used in this study matched the weight of the powder to be milled. The milling of powder was performed at a rotation speed of 200 rpm for a duration of 2 hours. Post mixing, the size of the FGM powder mixture was expected to be in range from 25 to 50 μm.

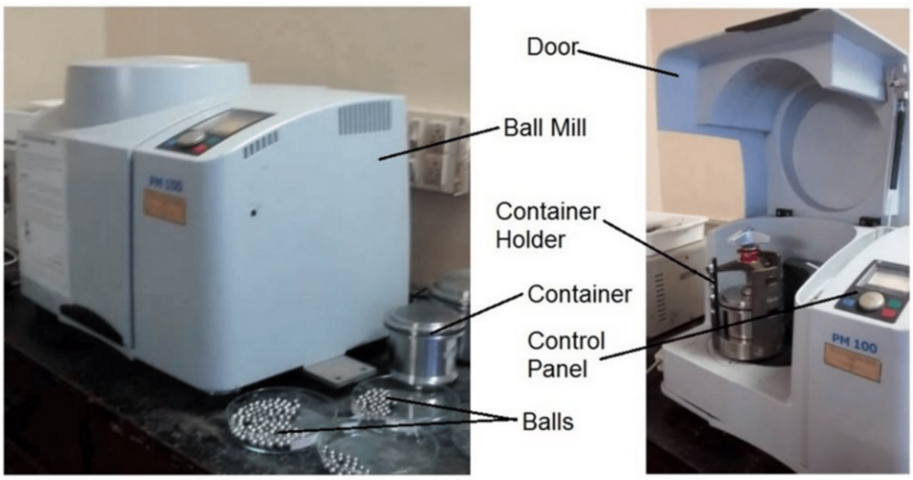

FIGURE 3: PM-100, Planetary Ball Mill used for blending FGM powders

FGM, functionally graded material

Plasma thermal spray process

The SUS316/Al_2O_3 system FGM samples were fabricated using the plasma spray process, also called as the flame/thermal spray process. This method is suitable for materials having melting temperatures higher than those achievable by the flame. The spray material is injected as a powder outside of the gun nozzle into the plasma plume, where it is melted, and hurled by the gas onto the substrate surface. The thermal spraying was performed using a Sulzer-Metco Atmospheric Plasma Spray system with a 3MB spraying gun, capable of up to 40 kW power. The cylindrical nozzle, made of copper, functions as the anode, while the cathode is composed of thoriated tungsten (containing 2 wt.% Thoria). The schematic of a typical plasma thermal spray gun is shown in Figure *4*. A 0.6 mm thick 100% pure SUS316 plate served as the substrate. The layers of molten powder material were carefully sprayed on this substrate. To prevent distortion during spraying, a steel backing plate was used to support the substrate. SUS316 substrate was brazed to the backing plate for support. Before thermal spraying, the SUS316 substrate surface was grit blasted with SiC grits to remove any rust, followed by cleaning with acetone. The FGM in powder form was melted in an oxy-acetylene flame to form a fine spray. The dry acetylene pressure was maintained at 1 kgf/cm^2 and oxygen pressure was set to 1.75 kgf/cm^2. To prevent metallurgical changes, damage, or distortion to the substrate, it was kept at a low temperature during the spraying process, allowing the molten droplets to solidify rapidly and form a coating. The FGM powder was carefully sprayed all over the substrate surface to ensure uniform thickness, with each layer maintained at approximately 0.1 to 0.2 mm. The thickness of each layer depended on the number of passes of the plasma spray gun, with each pass contributing roughly 0.075 to 0.1 mm to the layer thickness. The basic setup parameters used for fabrication of FGM beam samples are summarized in Table *2*. Three FGM beam samples, each with three layers, as detailed in Table *1*, were fabricated using similar process to assess the repeatability of the experimental results. In the fourth beam sample, 100% Al_2O_3 powder was sprayed onto the SUS316 substrate to compare the FG material coating with a pure ceramic coating on a metal substrate.

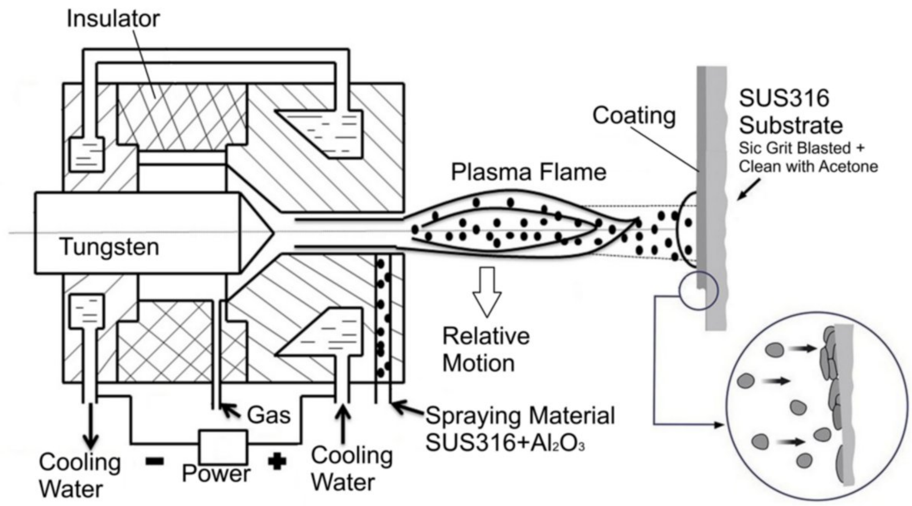

FIGURE 4: Schematic diagram of a typical plasma spray process

Parameters	GSP
Gas flow rate Ar/H_2	45/15 NL/min
Spray rate	3 kg/h
Particle velocity	≤450 m/s
Gas temperature	12000°C
Stand-off distance	100 mm
Substrate preheating temperature	200°C

TABLE 2: Plasma spraying setup parameters for FGM sample fabrication

FGM, functionally graded material; GSP, gas-stabilized plasma

Results

The microstructure analysis of SUS316 and Al_2O_3 powders, along with their mixtures of different compositions and metallographically polished FGM beam samples, was examined using a JEOL JSM

6380LA SEM. A SEM is a type of electron microscope that provides high-resolution, detailed images of the surface of a sample. SEM uses focused beams of electrons to scan the surface of a specimen which allows SEM to achieve much higher magnifications and resolutions, typically in the nanometer to micrometer range. An SEM images are highly useful for the study and characterization of FGMs. SEM provides detailed images at high magnifications, allowing the examination of the microstructure of FGMs. This is important because the properties of FGMs depend significantly on their microstructure, which changes across the material. SEM images are used to study the microstructure, phase distribution, surface morphology, porosity, and defects in FGMs. They help identify the gradation of materials, evaluate surface coatings, and measure the thickness of different layers. The samples for the current study were prepared using standard procedures for SEM analysis.

SEM analysis of powder and mixtures

SEM images of SUS316 powder as in Figure *5a* indicated that SUS316 powder composes of spherical particles with varying sizes of powder molecules from 3.22 μm to 36.6 μm. SEM micrograph of pure aluminium oxide is shown in Figure *5b*. Alumina particles have irregular flake-like structure with sharp and pointed edges, with particle sizes ranging from 13.9 μm to 72 μm. Figure *6* shows the SEM micrographs of SUS316-Al_2O_3 powder mixtures with compositions of SUS316 and Al_2O_3 in ratios of 60:40 and 80:20. It is observed that as the volume fraction of Al_2O_3 increases, a more pronounced flake-like structure emerges, with particle sizes ranging from 22.1 μm to 44.3 μm and SUS316 spherical particles with varying sizes of powder molecules from 4.12 μm to 21.2 μm.

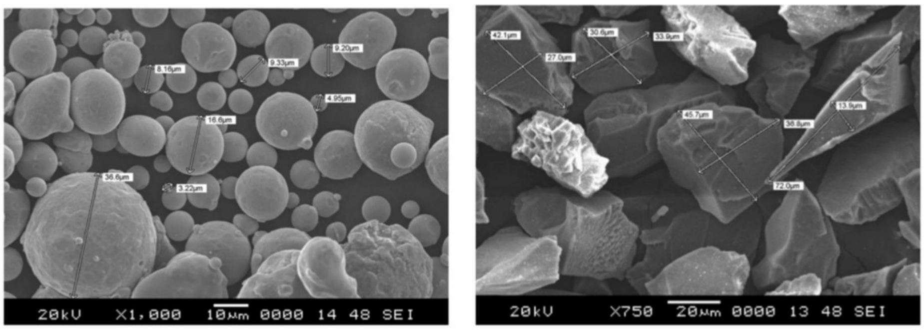

(a) (b)

FIGURE 5: SEM micrographs of (a) SUS316 powder and (b) aluminium oxide (Al2O3) powder

SEM, scanning electron microscopy

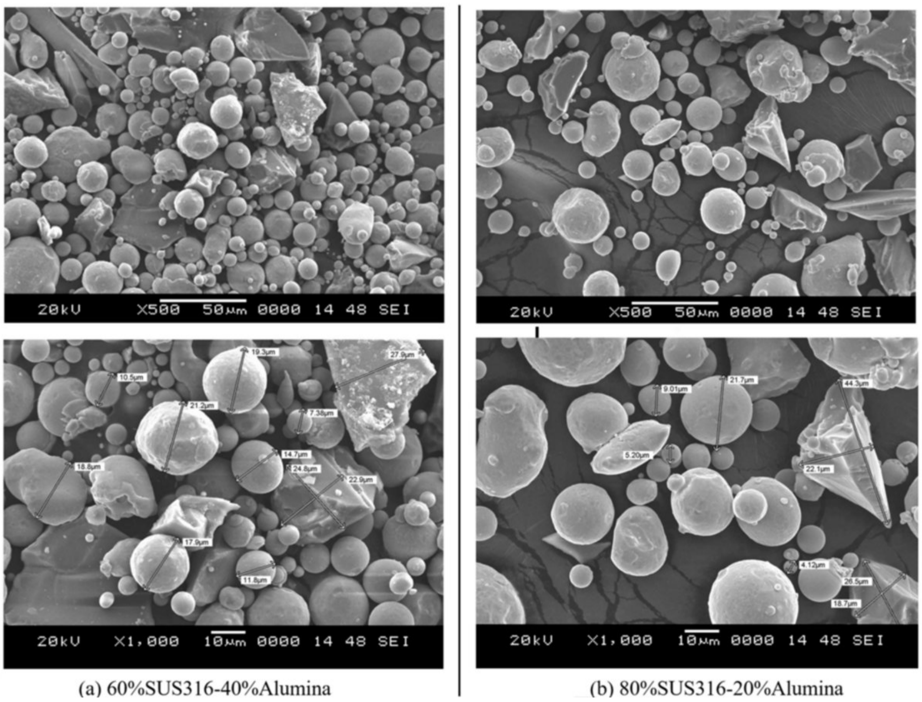

FIGURE 6: SEM micrographs of mixture of SUS316-Al2O3 powders

SEM, scanning electron microscopy

SEM analysis of FGM beam samples

Figure *7a* presents the SEM micrographs of the SUS316-Al_2O_3 FGM beam sample no. 2 across its thickness. The micrograph indicates that the material composition of stainless steel (SUS316) and aluminum oxide (Al_2O_3) varies across the thickness of the beam. A magnified view of the encircled area in the SEM micrograph is shown in Figure *7b*. In this image, it is observed that there is strong interface bonding between the FGM mixture and the SUS316 substrate, with only minor porosity or voids. The dark spots in the SEM micrograph correspond to aluminum-oxide particles, while the lighter, plain areas represent the SUS316 material.

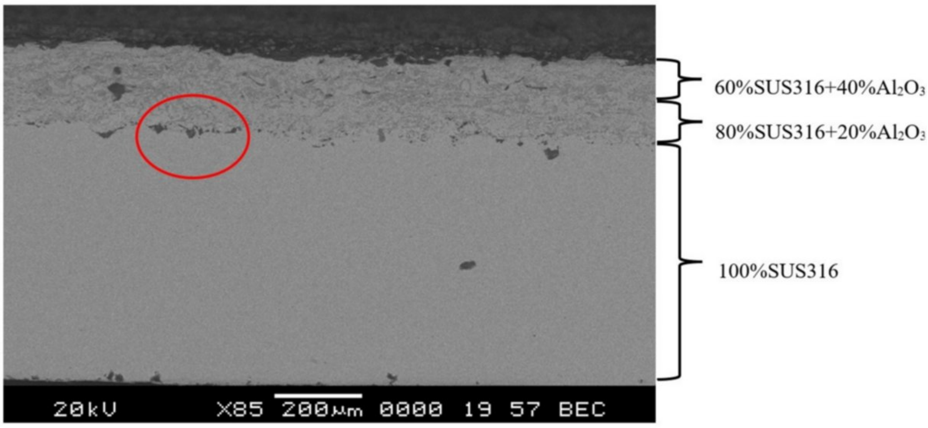

(a) variation of composition across thickness

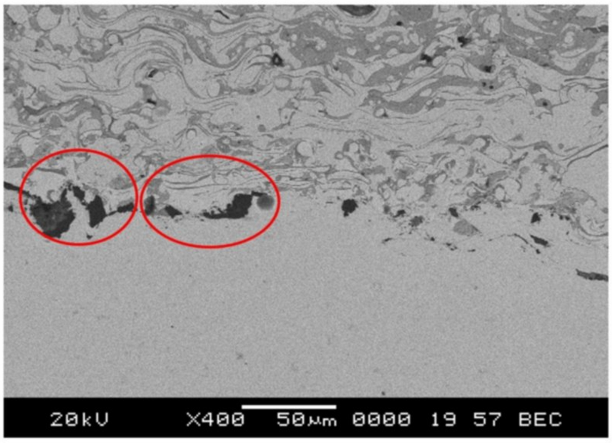

(b) interface of SUS316 substrate and SUS316-Al_2O_3 sprayed layer

FIGURE 7: SEM micrographs of thermal sprayed SUS316-Al2O3 FGM beam sample no. 2

SEM, scanning electron microscopy; FGM, functionally graded material

Discussion

The plasma thermal spray technique was successfully employed to fabricate FGM beams of SUS316 and Al_2O_3. Achieving a consistent compositional gradient required careful attention to beam design and material selection, including controlling the relative speed of the spray gun and adjusting the coating thickness to below 0.075 mm with each pass. A total of four FGM beams were successfully produced with three- and two-layer counts having outermost ceramic volume fractions as 40% and 100%, respectively. The microstructural study of the pure SUS316, alumina powders, and SUS316-Al_2O_3 powder mixtures using SEM, revealed clear morphological differences between SUS316 and alumina particles, which helped in distinguishing SUS316 and Al_2O_3 particles in the mixture. The SEM observations reveal that as the volume fraction of aluminum oxide increases, a more pronounced flake-like structure emerges, confirming the higher aluminum oxide content in the powder mixture, as seen in Figure *6*. Additionally, the SEM images demonstrate a uniform distribution of aluminum oxide within the SUS316 powders with varying particle size.

SUS316-Al_2O_3 FGM beams were successfully fabricated, with material gradation observed in all specimens. The microstructural analysis confirmed the uniform distribution of ceramic (darker grey spots) and metallic (lighter creamy areas) phases, indicating consistent gradation across the beams, as seen in Figure *8*. Defects such as porosity/voids (dark black areas) encountered during sample preparation were addressed by optimizing the processing parameters, leading to the production of high-quality FGM beams. It is observed that the Al_2O_3 is evenly distributed within the SUS316 matrix, illustrating a strong interfacial bonding. The interface between the 20% and 40% Al_2O_3 layers is difficult to distinguish in Figure *7a* due to the homogeneous compositions of SUS316-Al_2O_3 in adjacent layers. However, the bottom layer (100% SUS316 substrate) and the FGM top layer (60% SUS316 and 40% Al_2O_3) can be easily differentiated. The microstructure showed a smooth transition from metal-rich zones, consistent with the intended material gradation.

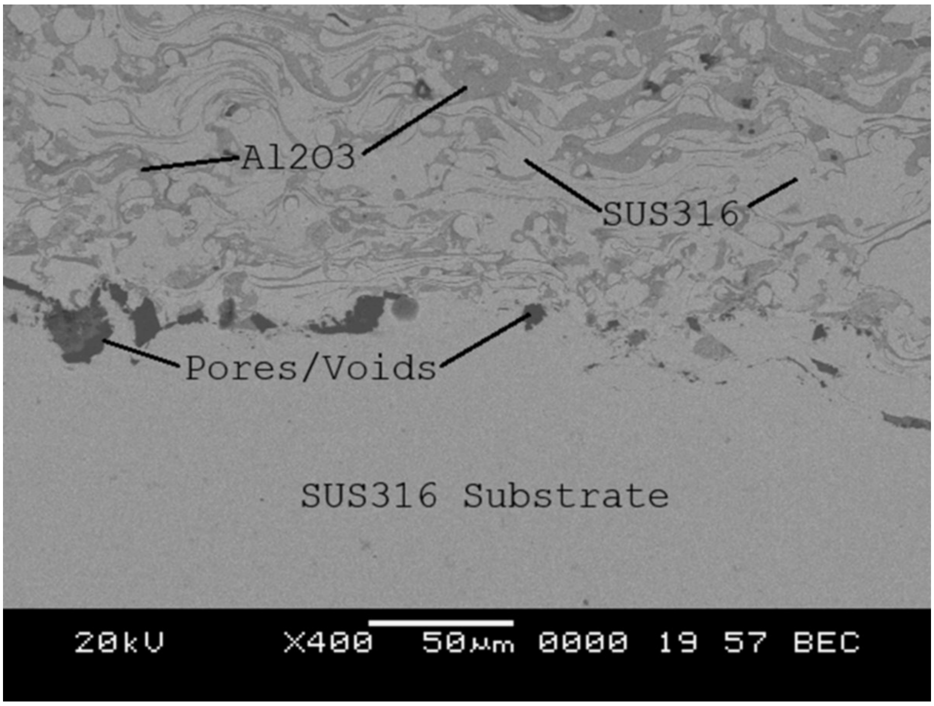

FIGURE 8: Distribution of SUS316 and Al2O3 in beam sample with defects

The study confirms that continuous material gradation is attainable, and optimization of process parameters effectively minimizes defects. These findings provide crucial insights into the successful fabrication of FGMs with controlled ceramic content and layered structures, offering a basis for further development in the manufacturing of advanced composite materials. This approach enabled a more continuous and customized distribution of alumina, significantly reducing thermal mismatch and improving structural integrity. The samples were further used for transient thermal analysis and thermo-elastic response of SUS316-Al_2O_3 FGM beam. The response of the two FGM beams were studied when subjected to localized varying heat loads. The experimental results indicate that SUS316-Al_2O_3 FGM beams experience elastic deflection under higher thermal loads. The detailed discussion on thermo-elastic response studies is not part of this article.

Conclusions

The plasma thermal spray technique has proven to be an effective method for producing SUS316-Al_2O_3 FGM beams. This study demonstrates that a continuous gradation of materials can be achieved, and that optimizing process parameters significantly reduces defects. These results offer valuable insights into the controlled fabrication of FGMs with tailored ceramic content and layered structures, laying the foundation for further advancements in the production of high-performance composite materials.

A microstructural analysis of pure SUS316, alumina powders, and their mixtures using SEM revealed distinct morphological differences between the SUS316 and alumina particles, enabling clear identification of each component within the mixed powders. The microstructural distribution of material along the beam thickness showed the gradation of Al_2O_3. It is observed that there is a good interface bonding of the SUS316-Al_2O_3 FGM mixture with the SUS316 substrate with minor porosity or voids. The material gradation studies of the beam will help the designer to opt for suitable power law index that will provide a compromise for appropriate functional requirements on the structural element as well as design variables like deflection and natural frequency.

The potential applications of FGMs are vast and unique, and they are expected to experience significant advancements in the near future due to their exceptional properties, which are difficult to replicate in conventional coatings. Despite rapid progress, particularly over the past decade, and numerous studies aimed at enhancing the use of FGMs with gradient structures in various engineering applications, many challenges remain. These include overcoming obstacles in scaling these coatings from laboratory-level research to industrial-scale production for several of the manufacturing methods discussed in this article.

Additional Information

Author Contributions

All authors have reviewed the final version to be published and agreed to be accountable for all aspects of the work.

Concept and design: Pravin Malik, Ravikiran Kadoli

Acquisition, analysis, or interpretation of data: Pravin Malik

Drafting of the manuscript: Pravin Malik

Critical review of the manuscript for important intellectual content: Pravin Malik, Ravikiran Kadoli

Supervision: Ravikiran Kadoli

Disclosures

Human subjects: All authors have confirmed that this study did not involve human participants or tissue. **Animal subjects:** All authors have confirmed that this study did not involve animal subjects or tissue. **Conflicts of interest:** In compliance with the ICMJE uniform disclosure form, all authors declare the following: **Payment/services info:** All authors have declared that no financial support was received from any organization for the submitted work. **Financial relationships:** All authors have declared that they have no financial relationships at present or within the previous three years with any organizations that might have an interest in the submitted work. **Other relationships:** All authors have declared that there are no other relationships or activities that could appear to have influenced the submitted work.

References

1. Naebe M, Shirvanimoghaddam K: Functionally graded materials: A review of fabrication and properties. Applied Materials Today. 2016, 5:223-45. 10.1016/j.apmt.2016.10.001
2. Gupta A, Talha M: Recent development in modeling and analysis of functionally graded materials and structures. Progress in Aerospace Sciences. 2015, 79:1-14. 10.1016/j.paerosci.2015.07.001
3. Isakeit D, Watillon P, Wilson A, Cazaux C, Bréard G, Leveugle T: The Atmospheric Reentry Demonstrator. European Space Agency. 1998, BR-138.
4. Lambros J, Narayanaswamy A, Santare M, Anlas G: Manufacture and testing of a functionally graded material. Journal of Engineering Materials and Technology. 1999, 121:488-93. 10.1115/1.2812406
5. Mahamood RM, Akinlabi ET, Shukla M, Pityana S: Functionally Graded Material: An Overview. Proceedings of the World Congress on Engineering. London, UK; 2012. Vol III:
6. Sobczak JJ, Drenchev L: Metallic functionally graded materials: a specific class of advanced composites. Journal of Material Science and Technology. 2013, 29:297-316. 10.1016/j.jmst.2013.02.006
7. Mondal K, Nuñez L, Downey CM, van Rooyen IJ: Recent advances in the thermal barrier coatings for extreme environments. Materials Science for Energy Technologies. 2021, 4:208-10. 10.1016/j.mset.2021.06.006
8. Ju Y, Li C, Yang X, Ba L, Wang Y, Di X: Recent progress on additive manufacturing of steel-based functionally graded materials. Materials Today Communications. 2024, 40:109953. 10.1016/j.mtcomm.2024.109953
9. Saleh B, Jiang J, Fathi R, et al.: 30 Years of functionally graded materials: An overview of manufacturing methods, applications and future challenges. Composites Part B Engineering. 2020, 201:108376. 10.1016/j.compositesb.2020.108376
10. Ctibor P, Ageorges H, Neufuss K, Zahalka F: Composite coatings of alumina-based ceramics and stainless steel manufactured by plasma spraying. Materials Science. 2009, 15:108-14.
11. Gu YW, Khor KA, Fu YQ, Wang Y: Functionally graded ZrO2-NiCrAlY coatings prepared by plasma spraying using pre-mixed, spheroidized powders. Surface and Coatings Technology. 1997, 96:305-12. 10.1016/s0257-8972(97)00185-0
12. Amsellem O, Borit F, Guipont V, Jeandin M, Pauchet F: A composite approach to Al2O3 based plasma-sprayed coatings. Proceedings of the 20th International conference on surface modification technologies, Vienne, Austria. 2007. 30-34.
13. Zhang J, Kobayashi A: Corrosion resistance of Al2O3+ZrO2 composite coatings sprayed on stainless steel substrates. Transactions of JWRI. 2005, 34:17-22.
14. Li CJ, Sun B: Microstructure and property of Al2O3 coating microplasma-sprayed using a novel hollow cathode torch. Materials Letters. 2004, 58:179-83. 10.1016/s0167-577x(03)00441-5
15. Kapuria S, Bhattacharyya M, Kumar AN: Bending and free vibration response of layered functionally graded beams: A theoretical model and its experimental validation. Composite Structures. 2008, 82:390-402. 10.1016/j.compstruct.2007.01.019
16. Malik P, Kadoli R: Nonlinear bending and free vibration response of SUS316-Al2O3 functionally graded plasma sprayed beams: theoretical and experimental study. Journal of Vibration and Control. 2016, 24:1171-184. 10.1177/1077546316659422
17. Bhattacharyya M, Kumar AN, Kapuria S: Synthesis and characterization of Al/SiC and Ni/Al2O3 functionally graded materials. Materials Science and Engineering A. 2008, 487:524-35. 10.1016/j.msea.2007.10.040
18. Wattanasakulpong N, Gangadhara PB, Kelly DW, Hoffman M: Free vibration analysis of layered functionally

graded beams with experimental validation. Materials & Design (1980-2015). 2012, 36:182-90. 10.1016/j.matdes.2011.10.049

19. Maitra K, Parihar RS: Finite element analysis of rotating truncated functionally graded conical shell. Current Materials Science. 2023, 16:62-71. 10.2174/2666145415666220516213438
20. Williams J, Hitchcock D, He J: Spark plasma sintering: a brief survey of recent patents. Recent Patents on Materials Science. 2012, 5:191-98. 10.2174/1874464811205030191
21. Grammes T, Mishra AK, Battalov K, Purwitasari A, Emmerich T, Aktaa J: Mechanical properties and quality of plasma sprayed, functionally graded tungsten/steel coatings after process upscaling. Materials Chemistry and Physics. 2024, 311:128530. 10.1016/j.matchemphys.2023.128530
22. Ortega-Bautista B, Henao J, Poblano-Salas C, et al.: Understanding the deposition of multilayered hydroxyapatite-bioactive glass/hydroxyapatite/titanium dioxide coatings on PEEK substrates by plasma spray. Surface and Coatings Technology. 2024, 494:131543. 10.1016/j.surfcoat.2024.131543
23. Audouarda L, Tsoutsouvaa M, Horezana M, et al.: Chemical and microstructural characterisation of HfO2-Y2O3 ceramics with high amount of Y2O3 (33, 40 and 50 mol. %) manufactured using spark plasma sintering. Journal of the European Ceramic Society. 2023, 43:2093-103. 10.1016/j.jeurceramsoc.2022.12.061
24. Kim SH, Lee H, Yeon SM, et al.: Selective compositional range exclusion via directed energy deposition to produce a defect-free Inconel 718/SS 316L functionally graded material. Additive Manufacturing. 2021, 47:102288. 10.1016/j.addma.2021.102288
25. Guo Z, Wang M, Wang Z, Wang F, Wang X, Huang J: Atmospheric plasma sprayed W coating/Detonation sprayed W-steel composite coating/steel substrate-based coating system for the tokamak first wall. Nuclear Materials and Energy. 2023, 35:101431. 10.1016/j.nme.2023.101431
26. Goudarzi ZM, Valefi Z, Zamani P: Effect of functionally graded structure design on durability and thermal insulation capacity of plasma-sprayed thick thermal barrier coating. Ceramics International. 2021, 47:34361-4379. 10.1016/j.ceramint.2021.08.349
27. Singh J, Chatha SS, Singh H: Synthesis and characterization of plasma sprayed functional gradient bioceramic coating for medical implant applications. Ceramics International. 2021, 47:9143-155. 10.1016/j.ceramint.2020.12.039
28. Muniraj D, Sreehari VM: Damage assessment of sandwich structures with Al/SiC functionally graded plasma sprayed faceplates subjected to single and repeated impacts. Composite Structures. 2022, 287:115369. 10.1016/j.compstruct.2022.115369
29. Matějíček J, Kavka T, Mušálek R, et al.: Tungsten-steel composites and FGMs prepared by argon-shrouded plasma spraying. Surface and Coatings Technology. 2021, 406:126746. 10.1016/j.surfcoat.2020.126746